**Supporting information**

**Multifunctional charge-transfer single crystals through supramolecular assembly**

By *Beibei Xu, Zhipu Luo, Andrew J. Wilson, Ke Chen, Wenxiu Gao, Guoliang Yuan, Harsh Deep Chopra, Xing Chen, Katherine A. Willets, Zbigniew Dauter, and Shenqiang Ren*[*]

Prof. S. R., Dr. B. X., Prof. H. D. C
Department of Mechanical Engineering and Temple Materials Institute
Temple University
Philadelphia, PA 19122, USA
E-mail: shenqiang.ren@temple.edu

Dr. Z. L., Prof. Z. D
Synchrotron Radiation Research Section
Macromolecular Crystallography Laboratory
National Cancer Institute
Argonne National Laboratory
Argonne, IL 60439, USA

A. J. W., Prof. K. A. W.
Department of Chemistry
Temple University
Philadelphia, PA 19122, USA

Dr. K. C.
Department of Physics and Temple Materials Institute
Temple University
Philadelphia, PA 19122, USA

W. G., Prof. G. Y.
School of Materials Science and Engineering
Nanjing University of Science and Technology
Nanjing, China

Dr. X. C.
Energy Systems Division
Argonne National Laboratory
Argonne, IL 60439, USA

**1. Synthesis of TTF-$C_{60}$ solution**

Three different kinds of schemes are used.

(1) For the crystal growth method without antisolvent, 25 mg/mL TTF was solved in acetonitrile (ACN), dimethylsulfoxide (DMSO) and hexane solvents, respectively. 25 mg/mL $C_{60}$ was solved in 1,2-dichlorobenzene (1,2-DCB) solvent. Then, TTF and $C_{60}$ solution were mixed with the volume ratio of 1:1 and stired at room temperature for 24 h.

(2) For the second scheme, 25 mg/mL $C_{60}$ was solved in 1,2-DCB solvent, and then TTF was added into the solution with the weight ratio of TTF:$C_{60}$ = 1:3, 2:3 and 3:3, and stired at room temperature for 24 h.

(3) For the third scheme, 10V% ACN, Ethanol (EtOH), Methanol (MeOH) was dropped into the solution made in the second scheme as antisolvents for $C_{60}$ and sonicated for 5 minutes at room temperature.

**2. Preparation of TTF-$C_{60}$ charge transfer crystals (TCCTs) devices**

Here, we use the solution prepared by the second scheme in part 1. For the preparation of amorphous devices, patterned ITO substrates were sonicated continuously in sofa water, distilled water, acetone and Iso Propyl Alcohol for 10 min and then blown dry by $N_2$. The substrates were then irradiated by oxygen plasma for 10 min. PEDOT:PSS was spun-coated on the substrates at a speed of 3600 rpm/min

for 1 min and dried at 150 $^{o}$C for 30 min. 25 mg/mL TTF/$C_{60}$ in 1,2-DCB solution was spun coated at 1000 rpm/min for 1 min. The devices were stay overnight. Then, the devices were annealed at 80 $^{o}$C for 10 min. 8 nm bathocuproine layer was deposited by thermal evaporation, followed by the deposition of 80 nm Aluminum electrodes.

For the preparation of cocrystal samples, the solution was drop-casted onto silica substrates and holded in sealed Teflon sample holder for 24 h. After forming cocrystals, carbon paste was pasted on two sides of the cocrystals with distance of 20 μm as the electrodes.

**3. Crystallization and morphology of the crystals**

Numerous methods have been developed for the preparation of TTF-based charge transfer-(CT) crystals, including solid-state reaction,[1,2] electric-field assisted thermal evaporation,[3] electrocrystallization,[4] and diffusion method.[5] As we can imagine, the scalable crystallization of a high quality CT complex is not an easy task. Moreover, most of these methods cannot get large dimensional crystals of high quality or spend long hours.

Due to the large difference of solubility for TTF and $C_{60}$ in other solvent besides 1,2-DCB, it always induces the rapid crystallization of $C_{60}$ and thereby affect the crystal growth without uniform cocrystals (Figure S1). The $C_{60}$ crystals are ribbon-like shape with the rough surface (Figure S2).

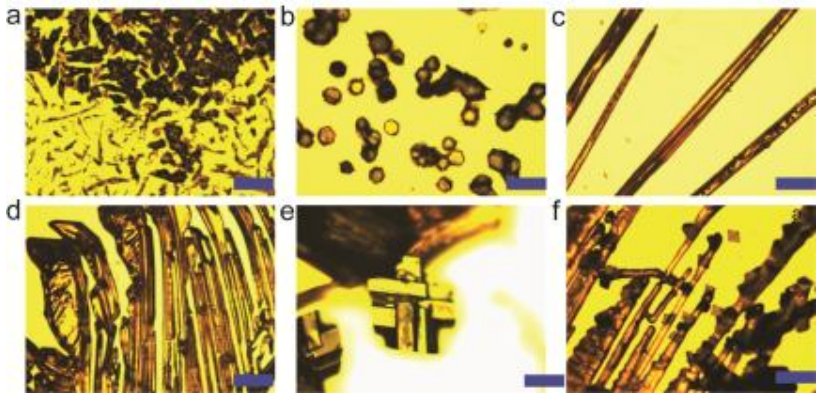


Figure S1. Optical microscopy (OM) images of the crystals. a-c, the solvents for TTF are DMSO, hexane and ACN, respectively. The solvents for $C_{60}$ are 1,2-DCB. d-f, The solvents for TTF/$C_{60}$ are all 1,2-DCB. The antisolvents are ACN, MeOH and EtOH, respectively. The scale bars are 50 μm.

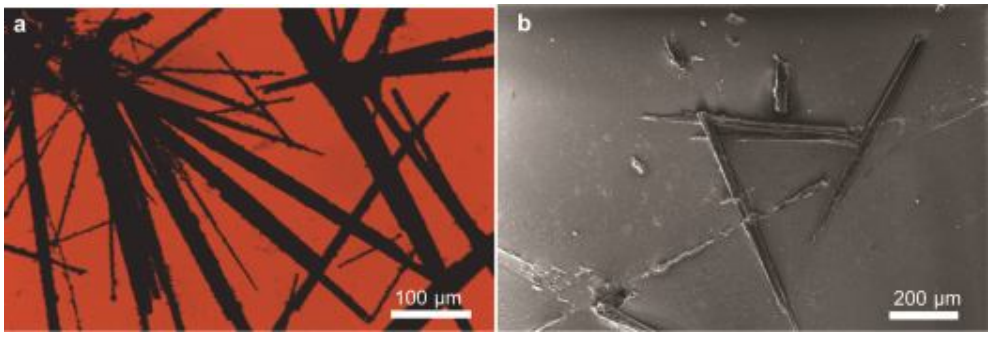


Figure S2. The OM images (a) and SEM images (b) of $C_{60}$ crystals at a concentration of 25 mg/mL.

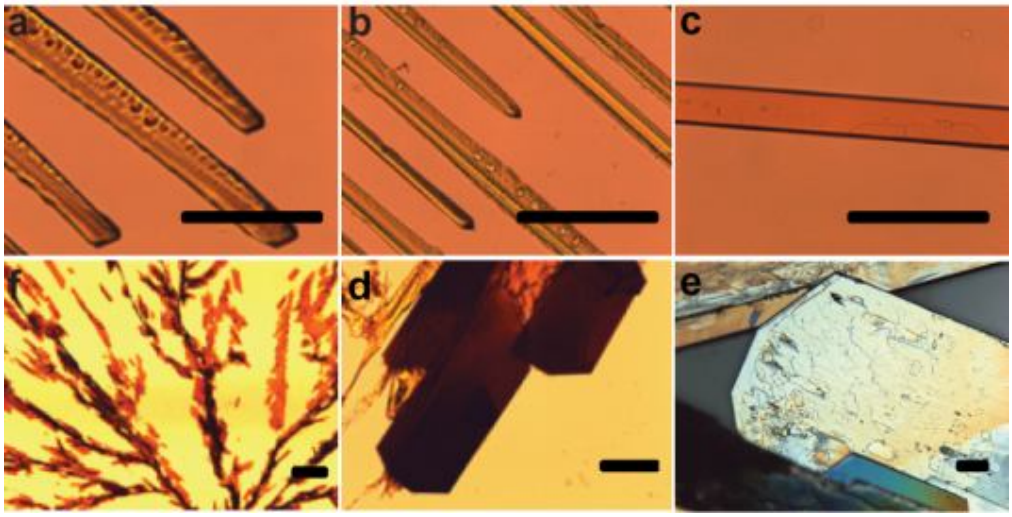


Figure S3 a-c, OM images of TTF single crystal. TTF concentrations are 8.3, 16.7 and 25 mg/mL, respectively. d-f, OM images of TCCTs. TTF concentrations are 8.3, 16.7 and 25 mg/mL, respectively. The $C_{60}$ concentration is maintained at 25 mg/mL. The scale bars are 50 μm, respectively.

Figure S4-S6 display TCCTs with the weight ratio of TTF:$C_{60}$ from 1:3, 2:3 to 3:3. The concentration of $C_{60}$ is all 25 mg/mL. TCCTs show quite different morphology from those of single component TTF or $C_{60}$ crystals. When the concentration of TTF:$C_{60}$ is 1:3, the morphology is dendritics with some plate-like thin crystals of dozens of micrometers in length and width on the branches and trunks (Figure S4). In comparison, for the weight ratio of TTF:$C_{60}$ as 2:3, the dendrites disappear with the appearance of stacking sheets of dozens to hundreds of micrometers in length and width (Figure S5). Much dense thicker plate-like crystals form at the highest concentration of TTF (Figure S6).

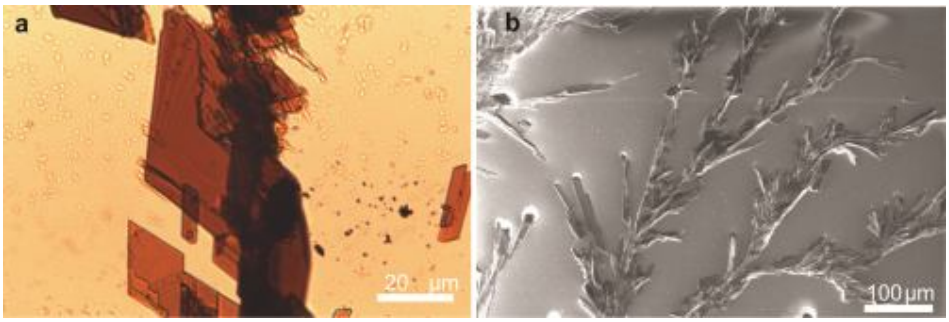


Figure S4. OM images (a) and SEM images (b) of TCCTs. The concentration of TTF is 8.3 mg/mL.

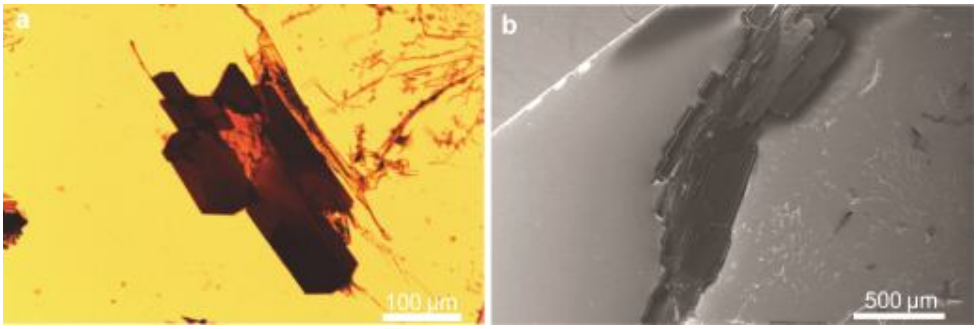


Figure S5. OM image (a) and SEM images (b) of TCCTs. The concentration of TTF is 16.7 mg/mL.

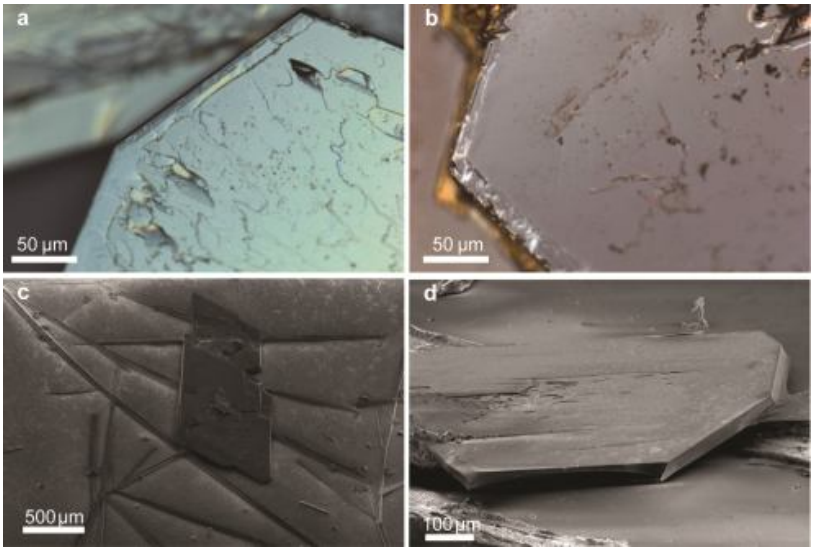


Figure S6. OM images (a, b), top view and cross-section SEM images(c, d) of TCCTs. The concentration of TTF is 25 mg/mL.

The yellow colored TTF single crystals grow into parallel aligned ribbon-like shape of centimeter-sized long and dozens of micrometers wide. At low concentration, the structure of TTF single crystals are very loose with some random void on the surface (Figure S7-S8). As the concentration increases, the structure becomes much denser with regular wrinkles on the surface (Figure S9).

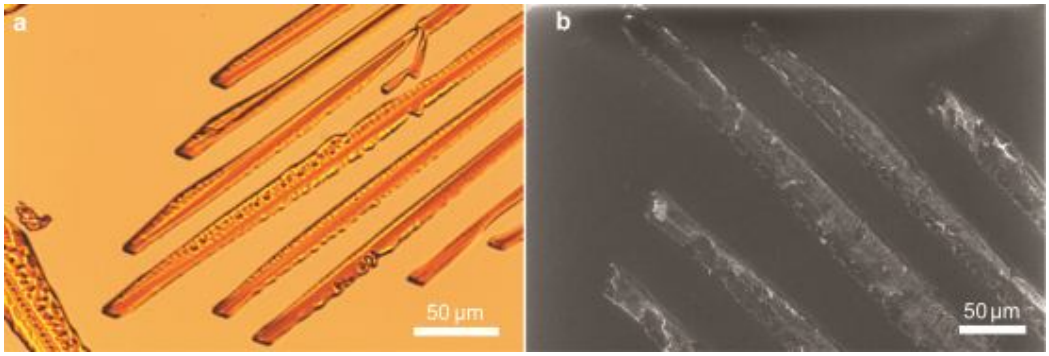


Figure S7. OM images (a, b) and SEM images (c, d) of TTF crystals at a concentration of 8.3 mg/mL.

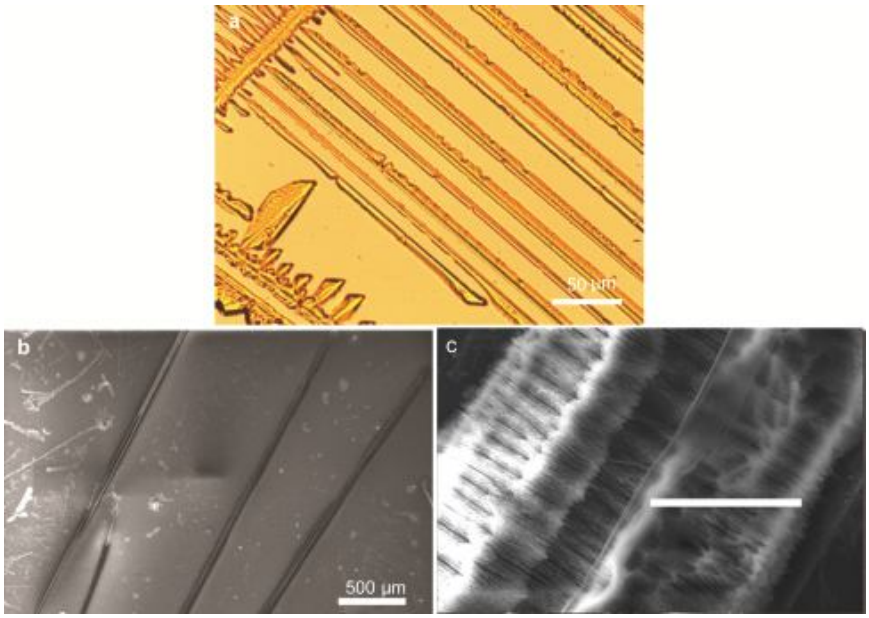


Figure S8. The OM image (a) and SEM images (b, c) of TTF crystals at a concentration of 16.7 mg/mL.

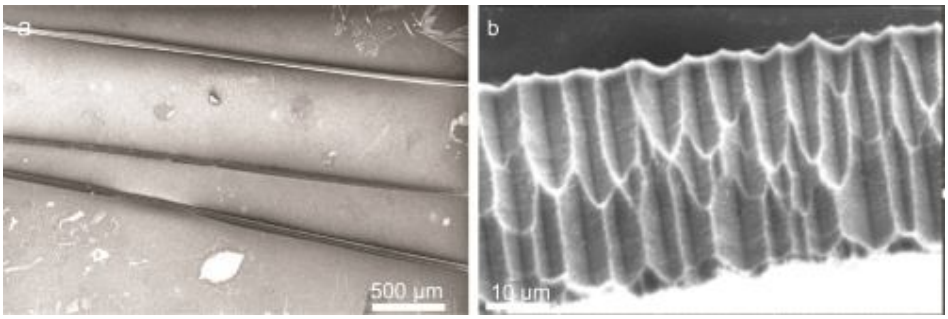


Figure S9. OM image (a) and SEM images (b, c) of TTF crystals at a concentration of 25 mg/mL.

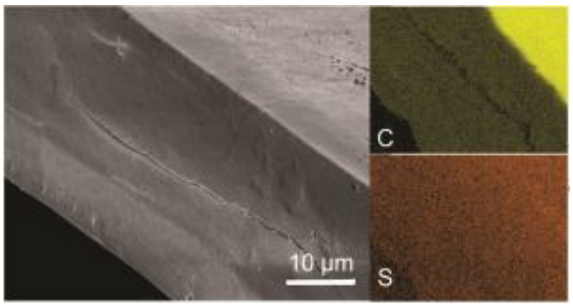


Figure S10. The SEM image and energy dispersive X-ray spectroscopy (EDS) element mapping for carbon and sulfur element.

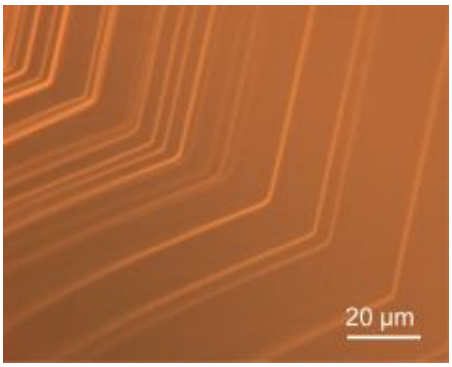


Figure S11. Polarized OM images of the edge for TCCTs showing layer by layer structure.

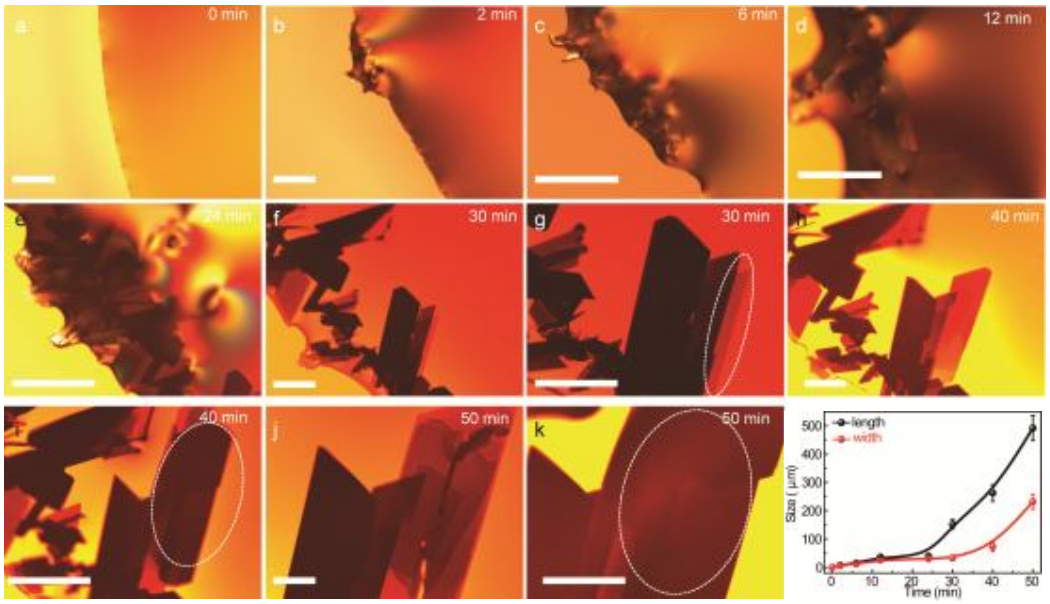


Figure S12. Time dependent in-situ OM images for the growth of TCCTs.

**4. Strucuture of the crystals**

Crystals were grown by adding TTF-$C_{60}$ solution on a 0.22 mm siliconized glass evaporated in an airtight container and appeared overnight. The TCCTs single crystal X-ray diffraction data, data collection and structure refinement details are summarized in Table S1-S3. A plate-like crystal was selected and pick up in the nylon loop and dipped into 3-methyl-1,5-pentanediol and then quickly cryo-cooled in a stream of cold nitrogen gas at SER-CAT 22-BM beamline at Advance Photon Source, Argonne National Laboratory, USA. Diffraction images were collected at wavelength of 0.8 Å with a MAR225 CCD detector. Data were integrated, scaled, and merged by *HKL-2000* (Otwinowski & Minor, 1997). The structure was solved by *SHELXT* (Sheldrick, 2015) and refined by *SHELXL* (Sheldrick, 2015) with final R factors: *R1*=4.3% for 22464 reflections [$F^2 > 2\sigma(F^2)$] and 2216 parameters.

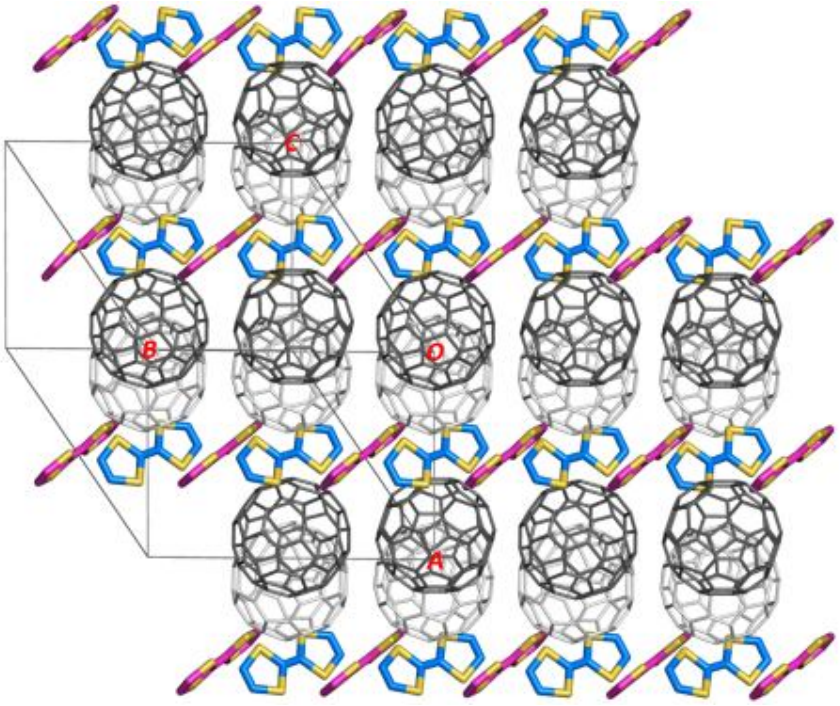


Figure S13. Packing structure of TCCTs.

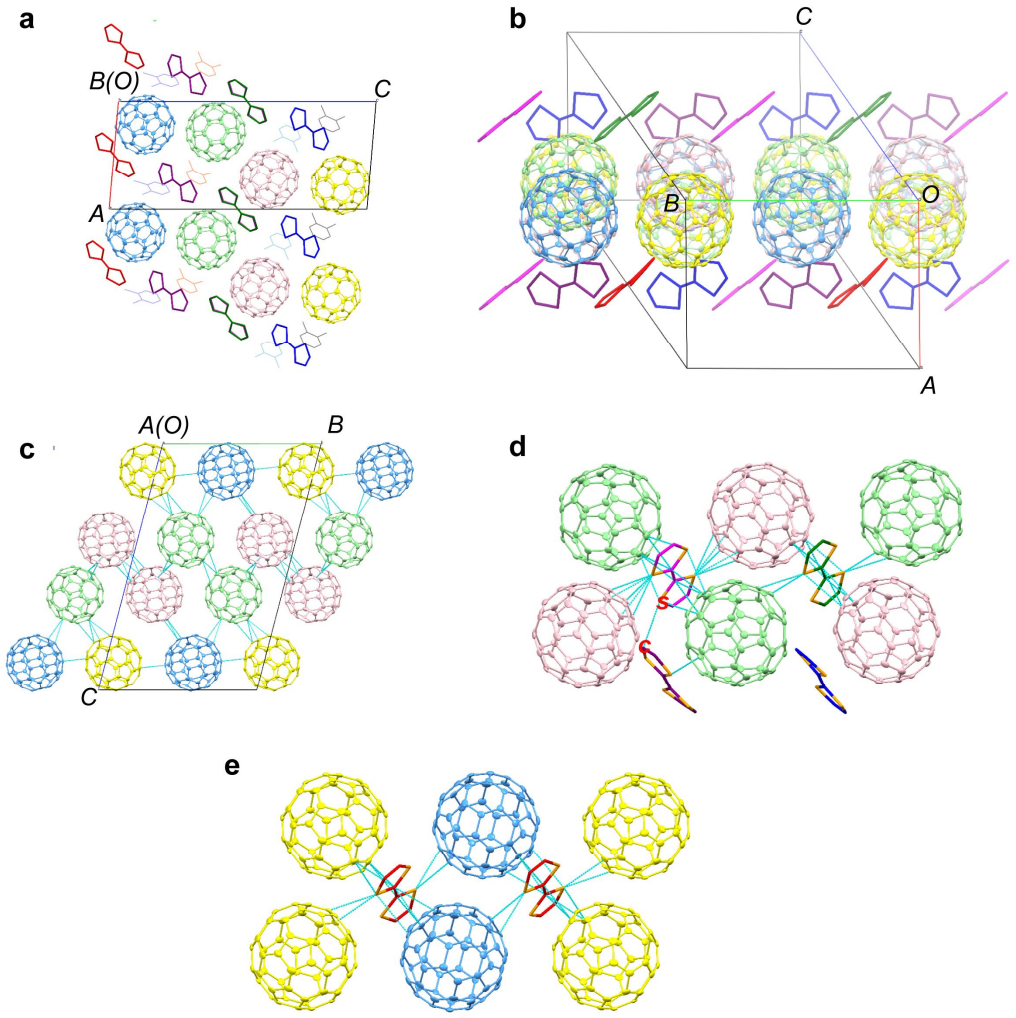


Figure S14. a, Projection of TCCTs crystal with segregated stacking structure along *b* axis. b, Perpendicular packing of two sets TTF molecules. Molecules are colored by symmetric equivalent. c, Intermolecular interaction between $C_{60}$ molecules. Molecules are colored by symmetric equivalents. d,e Intermolecular contacts of crystallographic nonequivalent TTF and adjacent $C_{60}$ molecules. $C(C_{60})\cdots S(TTF)$, $C(C_{60})\cdots C(TTF)$, and $C(TTF)\cdots S(TTF)$ are less than sum of the van der Waals radius of atoms are indicated. The Figs. c, d and e were drawn by *Mercury*,[49] The $C_{60}$ molecules are shown as ellipsoids, TTF are shown as sticks, DCBs are shown as wireframe. All molecules are colored by symmetric equivalents except the sulfur atoms are shown as gold in Figure S14d and S14e.

Table S1. Data of the crystal structure

| | |
|---|---|
| $4(C_{60})\cdot4(C_6H_4S_4)\cdot4(C_6H_4Cl_2)$ | $V$ = 8151 (3) Å$^3$ |
| $M_r$ = 4287.69 | $Z$ = 2 |
| Triclinic, $P\bar{1}$ | $F$(000) = 4304 |
| $a$ = 13.356 (3) Å | $D_x$ = 1.747 Mg m$^{-3}$ |
| $b$ = 20.269 (4) Å | Synchrotron radiation, λ = 0.8000 Å |
| $c$ = 31.853 (6) Å | μ = 0.58 mm$^{-1}$ |
| α = 103.95 (3)° | $T$ = 100 K |
| β = 91.70 (3)° | Plate, black |
| γ = 102.17 (3)° | 0.35 × 0.10 × 0.02 mm |
| *Data collection* | |
| MAR225 CCD diffractometer | 18767 reflections with $I > 2\sigma(I)$ |
| Radiation source: SER-CAT 22BM synchrotron beamline,APS,USA | $R_{int}$ = 0.0 |
| ω scans | $\theta_{max}$ = 26.4°, $\theta_{min}$ = 1.2° |
| Absorption correction: multi-scan *SCALEPACK* (Otwinowski et al., 2003) | $h$ = 0→14 |
| $T_{min}$ = 0.933, $T_{max}$ = 0.988 | $k$ = -22→22 |
| 22464 measured reflections | $l$ = -35→35 |
| 22464 independent reflections | |
| *Refinement* | |
| Refinement on $F^2$ | 8035 restraints |
| Least-squares matrix: full | Hydrogen site location: inferred from |

| | |
|---|---|
| | neighbouring sites |
| $R[F^2 > 2\sigma(F^2)] = 0.043$ | H-atom parameters constrained |
| $wR(F^2) = 0.131$ | $w = 1/[\sigma^2(F_o^2) + (0.0914P)^2 + 1.8666P]$ where $P = (F_o^2 + 2F_c^2)/3$ |
| $S = 1.07$ | $(\Delta/\sigma)_{max} = 0.002$ |
| 22464 reflections | $\Delta_{max} = 0.51$ e Å$^{-3}$ |
| 2216 parameters | $\Delta_{min} = -0.48$ e Å$^{-3}$ |

Table S2. Short intermolecular contacts less than the sum of van der Waals radius of atoms.

| Atom1 | Atom2 | Length (Å) | Length-VdW(Å) |
|---|---|---|---|
| C157 | C225 | 2.915 | -0.485 |
| C352 | C423 | 2.937 | -0.463 |
| C328 | C328 | 3.01 | -0.39 |
| C4 | C114 | 3.019 | -0.381 |
| C21 | C247 | 3.032 | -0.368 |
| C207 | C331 | 3.078 | -0.322 |
| C252 | C252 | 3.107 | -0.293 |
| C352 | C440 | 3.139 | -0.261 |
| C141 | C460 | 3.155 | -0.245 |
| C24 | C314 | 3.164 | -0.236 |
| C3 | C114 | 3.178 | -0.222 |
| C24 | C335 | 3.186 | -0.214 |
| C147 | C434 | 3.223 | -0.177 |
| S16 | C224 | 3.229 | -0.271 |
| C252 | C258 | 3.241 | -0.159 |
| C122 | C225 | 3.261 | -0.139 |
| C157 | C210 | 3.265 | -0.135 |
| C253 | C258 | 3.283 | -0.117 |
| S16 | C206 | 3.312 | -0.188 |
| C207 | C305 | 3.324 | -0.076 |
| C107 | C320 | 3.325 | -0.075 |
| S16 | C255 | 3.342 | -0.158 |
| C328 | C341 | 3.347 | -0.053 |
| C21 | C259 | 3.362 | -0.038 |
| C352 | C406 | 3.372 | -0.028 |
| S13 | C302 | 3.376 | -0.124 |

| | | | |
|---|---|---|---|
| S13 | C303 | 3.379 | -0.121 |
| C212 | C305 | 3.379 | -0.021 |
| S2 | C427 | 3.381 | -0.119 |
| C3 | C118 | 3.386 | -0.014 |
| C342 | C440 | 3.386 | -0.014 |
| C150 | C320 | 3.389 | -0.011 |
| S15 | C314 | 3.404 | -0.096 |
| S2 | C420 | 3.409 | -0.091 |
| S2 | C134 | 3.443 | -0.057 |
| S13 | C259 | 3.458 | -0.042 |
| C13 | S15 | 3.477 | -0.023 |
| S15 | C335 | 3.481 | -0.019 |
| S16 | C220 | 3.484 | -0.016 |
| S16 | C230 | 3.496 | -0.004 |

* C1 - C100 corresponds to the carbon atoms of TTF molecules. Four different kinds of $C_{60}$ molecules exist in the crystal lattice, classifying as C100 - C160, C200 - C260, C300 - C360, and C400 - C460 with different colors as shown in Fig. S15 and Tab. S2.

## 5. Optical properties of TCCTs

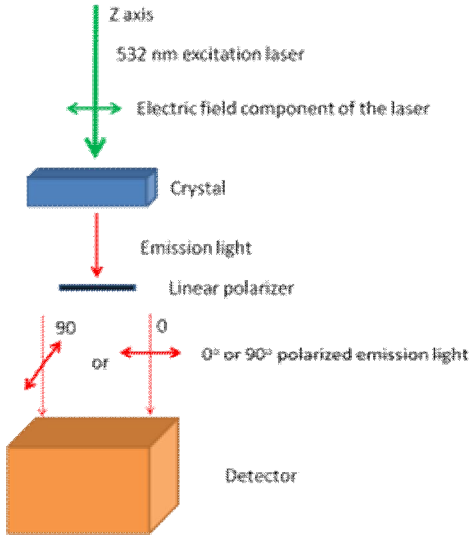


Figure S15. Measurement scheme of the angle dependent photoluminescence spectra.

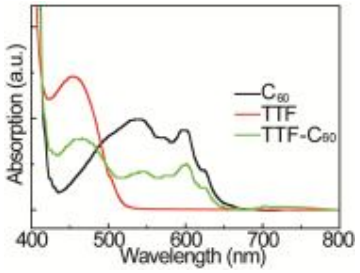


Figure S16. Absorption spectra of TTF, $C_{60}$ and in TTF-$C_{60}$ amorphous phase in 1,2-DCB solution.

Electrical potential dependent photoluminescence spectra are demonstrated in the main text and Figure S17. By increase the electrical potential, the emission intensity decrease. It then increases again with the decrease of the electrical potential showing reversible properties.

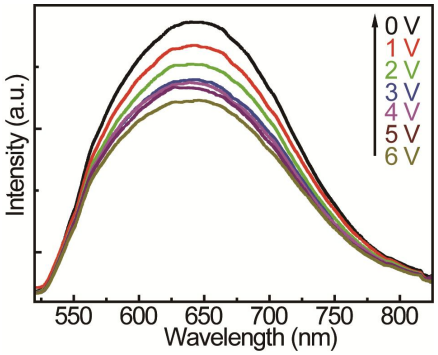


Figure S17. Potential dependent photoluminescence spectra for emission polarized at $0^{o}$ relative to the excitation polarization. The potential decreases from 6 V to 0 V.

**6. Electric properties, magneto-conductance (MC) of TCCTs and TTF-$C_{60}$ amorphous phase**

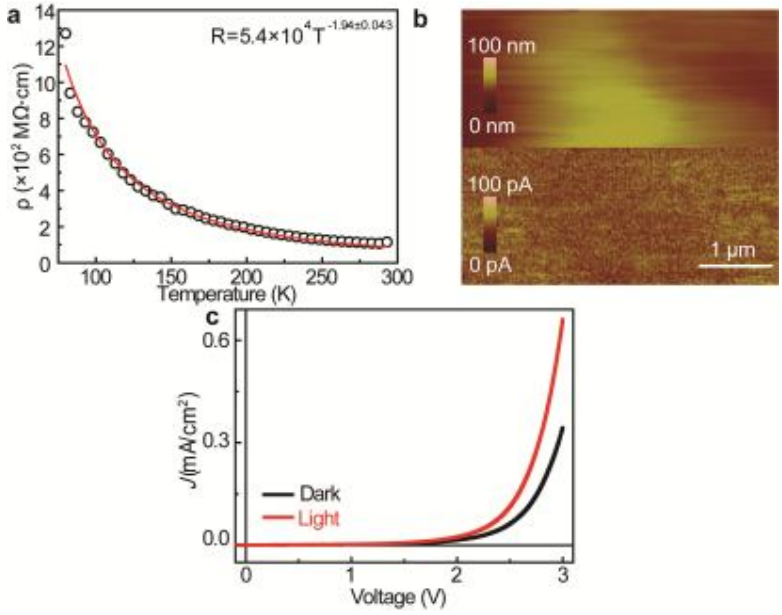


Figure S18. **a,** Temperature dependent resistivity along the c axis. **b,** AFM and conducting-AFM of TCCTs. **c,** Dark and light current-voltage curves under continuous sweeping of the voltage at a rate of 0.1 V $s^{-1}$. The source is a simulated solar light.

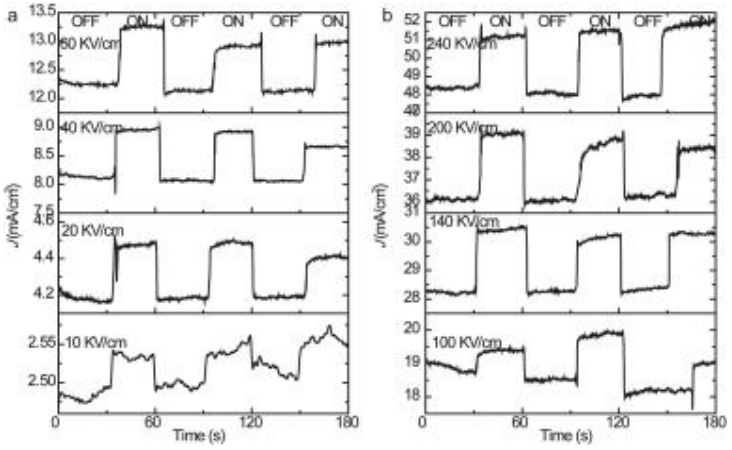


Figure S19. MC under different electric field of TCCTs. The magnetic field is 400 mT.

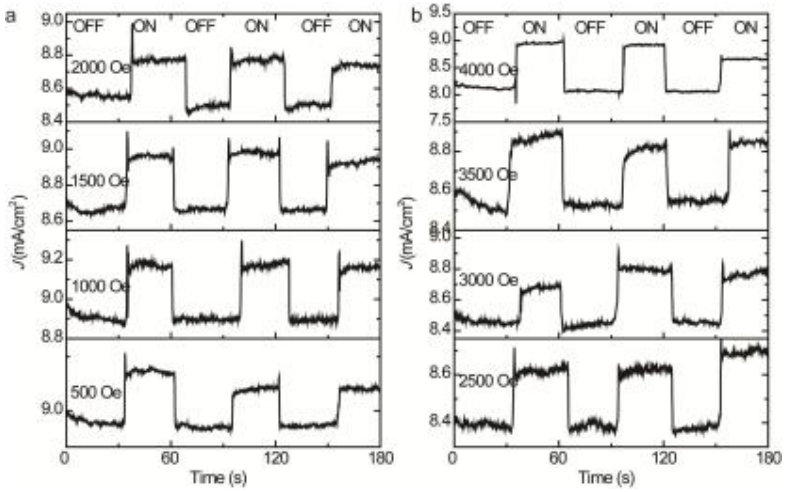


Figure S20. Magnetic field dependent MC of TCCTs. The electric field is 40 KV/cm.

**7. Polarization characteristic**

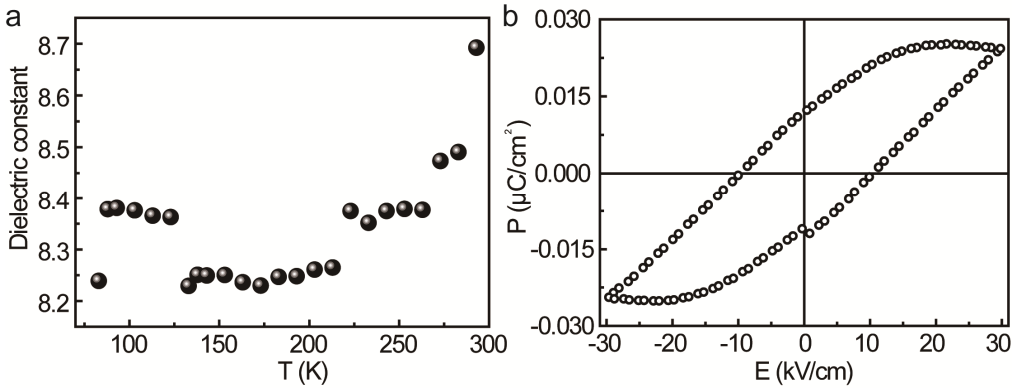


Figure S21. a, Temperature dependent dielectric constant change at 1 MHz. b, Polarization hysteresis loop at room temperature.

Piezoelectric force microscopy (PFM) was used to verify the ferroelectric properties in TCCTs. In Figure S22, by consecutively tuning the polarized electric field, obvious phase change was observed.

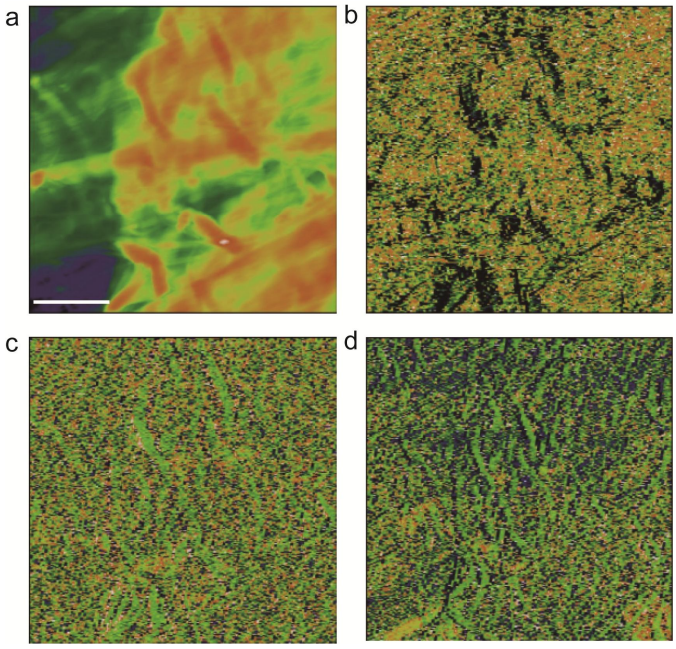


Figure S22. The height (a, topography) image of TCCTs and PFM images (b-d), and the tip bias voltage of -45, 10 and 90 kV/cm. The scale bar is 5 μm.

## 8. Electron spin resonance (ESR)

The $C_{60}$ single component shows a sharp peak with signal at g = 2.0000 (peak 2), which originates from oxygen-$C_{60}$ pair related $C_{60}^{-\cdot}$ radical anion.[6, 7] TTF single component gives a broad peak with signal at g=2.0046 (peak 1), which could be ascribed to $TTF^{+}$-related radicals.[6, 7] In comparison, TCCTs have three peaks with signals at g=2.0046, 2.0000, and 1.9959 (peak 3), respectively. The third signal at g=1.9959 indicates the CT state in the CTCs.

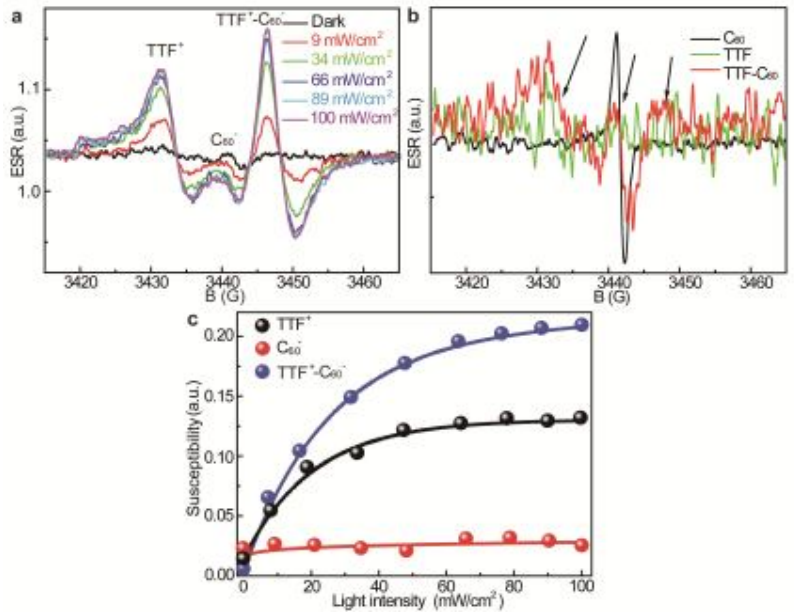


Figure S23. **a,** Susceptibility under different light intensities at 80 K. **b,**The ESR spectra of $C_{60}$, TTF and TCCTs at 80 K. **c,** Light intensity dependent susceptibility change at 80 K.

## 9. Magnetic characteristics

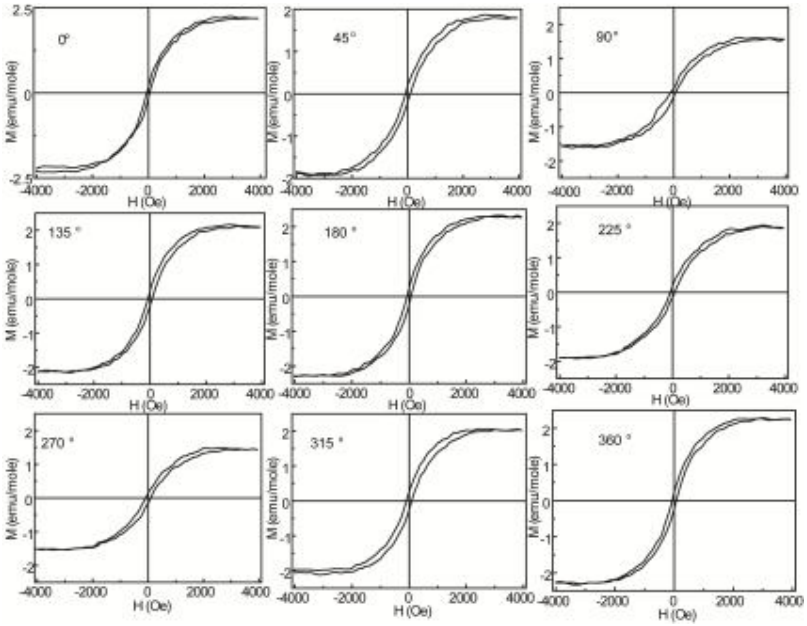


Figure S24. Angle dependent magnetic hysteresis (M-H) loops of TCCTs.

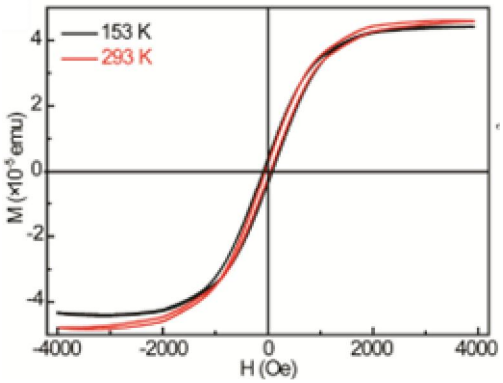


Figure S25.The M-H loops at room temperature and 153 K.

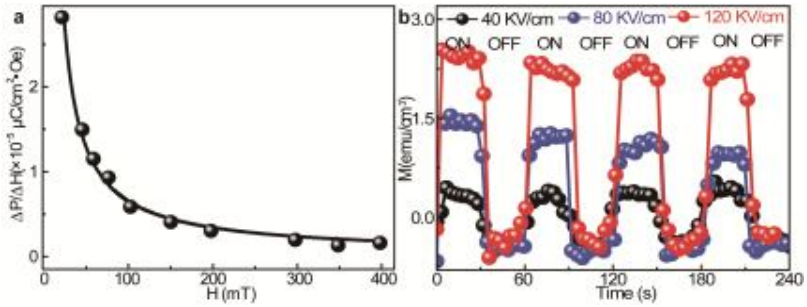


Figure S26. **a,** Indirect magnetoelectric coupling coefficient change as a function of magnetic field. **b,** Electric field tuning of magnetization of TCCTs.

**References**:

[1] J. Xiao, Z. Yin, H. Li, Q. Zhang, F. Boey, H. Zhang, Q. Zhang, *J. Am. Chem. Soc.* **2010**, *132*, 6926.

[2] J. P. Farges, A. Brau, *Phys. B+C* **1986**, 143, 324.

[3] M. Sakai, *J. Appl. Phys.* 2013, 113, 153513.

[4] L. Ren, X. Xian, K. Yan, L. Fu, Y. Liu, S. Chen, Z. Liu, *Adv . Funct. Mater.* **2010**, *20*, 1209.

[5] Anzai, H. *J. Cryst. Growth*. **1976**, 33, 185.

[6] J. Llacay, J. Veciana, J. Vidal-Gancedo, J. L. Bourdelande, R. González-Moreno, C. Rovira, *J. Org. Chem.* **1998**, *63*, 5201.

[7] K. B. Simonsen, V. V. Konovalov, T. A. Konovalova, T. Kawai, M. P. Cava, *J. Chem. Soc., Perkin Trans.* **1999**, *2*, 657.